104 (2025) 105068

Contents lists available at ScienceDirect

Poultry Science

journal homepage: www.elsevier.com/locate/psj

Full-Length Article

miR-200b-3p affects the proliferation and differentiation of chicken preadipocytes by modulating *SESN1* expression through competition with CircADGRF5

Pengtao Yuan [a,1], Hongtai Li [a,1], Hongyuan Zhang [a], Shengxin Fan [a], Yaqi Dai [a], Jiyu Jia [a], Jingqi Shen [a], Yanhua Zhang [a], Hong Li [a], Guirong Sun [a], Xiaojun Liu [a], Yadong Tian [a], Xiangtao Kang [a], Yinli Zhao [b,1,*], Guoxi Li [a,1,*]

[a] *The Shennong Laboratory, Henan Agricultural University, Zheng Zhou, Henan Province, 450046, PR China*
[b] *College of Biological Engineering, Henan University of Technology, Zheng Zhou, Henan Province, 450001, PR China*

ARTICLE INFO

Keywords:
miR-200b-3p
circADGRF5
SESN1;Preadipocytes
ceRNA network

ABSTRACT

Excessive deposition of abdominal fat in chickens has a significant impact on the poultry industry, and there is increasing evidence that non-coding RNAs play a crucial role in fat development. In our previous RNA-seq study, miR-200b-3p was found to be differentially expressed during different developmental periods of fat in Gushi chickens. In this study, we report that miR-200b-3p can directly bind to the 3′UTR region of *SESN1* to promote proliferation and inhibit differentiation of preadipocytes. Overexpression of *SESN1* inhibits preadipocyte proliferation and promotes differentiation. In contrast, inhibition of *SESN1* resulted in the opposite outcome. Interestingly, we also identified the circADGRF5/miR-200b-3p/*SESN1* ceRNA network involved in the developmental process of preadipocytes. Furthermore, we validated a novel circRNA, circADGRF5, in this report and found that it regulates *SESN1* expression through competitive binding with miR-200b-3p. In conclusion, these data suggest that miR-200b-3p directly targets *SESN1* to regulate the proliferation and differentiation of preadipocytes, and circADGRF5 regulates *SESN1* expression through competitive binding with miR-200b-3p.

Introduction

Chicken meat and eggs are among the most important sources of animal protein for humans. With the rapid development of the poultry industry in recent years, large-scale and intensive farming practices have led to numerous problems, such as excessive accumulation of abdominal fat. Studies have shown that the excessive accumulation of abdominal fat not only results in feed waste but also affects meat quality, egg production rates, and overall economic efficiency of the poultry industry. It may even pose health risks to human health (Baéza and Le Bihan-Duval, 2013; Milićević et al., 2014). Therefore, elucidating the molecular mechanisms underlying the development of abdominal fat tissue in chickens is of great significance for genetic breeding and production guidance in poultry.

Fat deposition is a complex, multistage physiological process influenced by nutritional conditions, environmental factors, and genetic factors. It also involves the coordinated regulation of various pathways, hormones, and transcription factors within the body (Moreira et al., 2018; Davoli et al., 2016). MicroRNAs (**miRNAs**) are a class of small non-coding RNAs, approximately 22 nucleotides (**nt**) in length, discovered in eukaryotes and viruses. They can pair completely or incompletely with the 3′ untranslated region (**3′-UTR**) of specific messenger RNAs (**mRNAs**), leading to the inhibition or degradation of mRNAs, thus regulating various developmental and cellular processes in eukaryotes (Song et al., 2011; O'Rourke et al., 2006; Ambros V., 2004; Bartel DP., 2004). Numerous studies have demonstrated that miRNAs are involved in the biological processes of adipose tissue development, including adipogenesis, adipocyte proliferation and differentiation, and lipid metabolism (Price et al., 2016). The first miRNA found to regulate lipid metabolism was miR-14 in Drosophila, whose deletion leads to an

The appropriate scientific section for the paper: Genetics and Molecular biology

* Corresponding author at: 218 Ping an Avenue, Zhengdong New District, Henan Agricultural University, Zhengzhou, 450046, PR China.
E-mail addresses: zhaoyl7322@126.com (Y. Zhao), liguoxi0914@126.com (G. Li).

[1] These authors contributed equally.

https://doi.org/10.1016/j.psj.2025.105068
Received 2 December 2024; Accepted 18 March 2025
Available online 19 March 2025

increase in triglyceride (**TG**) levels (Xu et al., 2003). miR-33 regulates lipid homeostasis and cholesterol metabolism by targeting genes involved in cholesterol transport and reduces fatty acid degradation by targeting genes associated with fatty acid β-oxidation in the liver (Shao et al., 2014). An increasing number of miRNAs are being discovered to play roles in the growth and development of adipose tissue, providing further insights into the molecular mechanisms of adipogenesis and lipid metabolism.

Circular RNAs (**circRNAs**) are a class of single-stranded, covalently closed non-coding RNAs generated by back-splicing from precursor mRNAs. They are widely present in eukaryotes, and many circRNAs are highly conserved during evolution (Patop et al., 2019; Liu et al., 2022). The potential mechanisms by which circRNAs exert their biological functions primarily involve interactions with other molecules. Numerous studies have shown that circRNAs act as molecular sponges for miRNAs, participating in post-transcriptional regulation. By competitively binding to miRNAs, they relieve the miRNA-mediated repression on target genes, thereby regulating gene expression, a mechanism known as competing endogenous RNAs (**ceRNAs**) (Panda AC., 2018). For instance, CircRNA_09505 can act as a sponge for miR-6089, regulating inflammation in CIA mice through the miR-6089/AKT1/NF-κB axis (Yang et al., 2020). CircNFIC promotes inflammation and apoptosis in chicken macrophages (**HD11**) via the miR-30e-3p/DENND1B axis (Chen et al., 2021), and circFGFR2 enhances the proliferation and differentiation of skeletal muscle myoblasts by targeting miR-29b-1-5p and miR-133a-5p (Chen et al., 2018). These studies contribute to our understanding of the roles of circRNAs in chicken growth and development. However, many aspects remain to be elucidated, especially the expression characteristics of circRNAs in the development of chicken adipose tissue and the biological functions of circRNAs associated with abdominal fat deposition.

In this study, based on previous high-throughput sequencing data, we found that miR-200b-3p is significantly differentially expressed during various stages of abdominal fat development in Gushi chickens (Chen et al., 2019). Further investigation revealed an interaction between the circular RNA derived from ADGRF5 (gga-circ_0005175, named circADGRF5), miR-200b-3p, and SESN1, which is involved in the development or deposition of abdominal fat in chickens. Therefore, this study aims to explore the interaction and biological functions of circADGRF5/miR-200b-3p/SESN1, thereby enhancing our understanding of the genetic basis and molecular mechanisms influencing abdominal fat deposition in poultry.

Materials and methods

Ethics statement

All experimental animals used in this study were sourced from the Animal Center of Henan Agricultural University and were raised under identical environmental conditions, with access to the same food and water. All animal experimental procedures were approved by the Institutional Animal Care and Use Committee of Henan Agricultural University (Permit Number: 11-0085). To ensure animal welfare, every effort was made to humanely euthanize the experimental animals.

Experimental animals and sample preparation

Gushi chicken is a dual-purpose local breed in China known for its tender meat, excellent flavor, tolerance to rough feed, and stable genetic traits. It is frequently used as a breeding material for high-quality meat chickens (Fu et al., 2018). Six healthy 6-week-old Gushi chickens were selected for the study. Under sterile conditions, samples of the heart, liver, spleen, lung, kidney, breast muscle, leg muscle, subcutaneous fat, and abdominal fat tissue were collected post-dissection. The tissues were cut into soybean-sized pieces and placed in 1.5 mL RNAase-free EP tubes, rapidly frozen in liquid nitrogen, and stored at -80°C for later use.

Isolation of primary preadipocytes

14-day-old Gushi chickens reared under standard conditions were aseptically sacrificed, followed by surface disinfection with 75 % ethanol. Abdominal adipose tissue was dissected in a laminar flow hood, rinsed three times with PBS to remove vascular fascia, and minced into fragments. Tissue fragments were digested in collagenase solution (1:5 tissue-to-solution ratio) at 37°C for 60 minutes with intermittent shaking every 5 minutes. Digestion was terminated by adding complete culture medium, and the mixture was sequentially filtered through 100-, 200-, and 500-μm mesh sieves. The filtrate was centrifuged at 1,500–2,000 ×g for 10 min, after which the supernatant was discarded. Pelleted cells were resuspended in erythrocyte lysis buffer for 10 minutes, centrifuged under identical conditions, and washed twice with PBS. Cells were finally resuspended in complete medium and cultured in a humidified incubator at 37°C with 5 % CO_2.

Cell culture

The chicken embryonic fibroblast cell line (**DF-1**) was a cell line preserved by our research group. Chicken preadipocytes were isolated following previously established methods (Zhai et al., 2023). Both chicken preadipocytes and DF-1 cells were cultured in Dulbecco's Modified Eagle's Medium F12 (**DMEM-F12**), supplemented with 10 % fetal bovine serum (FBS, BI, Israel) and 1 % penicillin-streptomycin. The cells were maintained in a cell culture incubator at 37°C with 5 % CO2.

Induced differentiation

Preadipocytes were seeded into 6-well cell culture plates. When the cell density reached 90 %, the complete medium was replaced with induction differentiation medium, which was then changed every 48 hours. Cell samples were collected at 0d, 1d, 2d, 3d, 4d, and 5d, with three biological replicates for each time point. Oleic acid stock solution was prepared by dissolving 6.3 μL of oleic acid standard in 1 mL of DMSO. The induction differentiation medium was then prepared by mixing 800 μL of oleic acid stock solution with 100 mL of complete medium (Shang et al., 2014).

Oil Red O staining

Preadipocytes were washed three times with phosphate-buffered saline (**PBS**) and fixed with 10 % paraformaldehyde for 30 minutes. After washing again three times with PBS, the cells were stained with Oil Red O (Sigma, St. Louis, MO, USA) dissolved in 100 % isopropanol at room temperature for 30 minutes. The cells were then rinsed with 60 % isopropanol for 10 seconds, washed three times with PBS, and imaged under a microscope. After imaging, the intracellular Oil Red O was dissolved with 100 % isopropanol for 5 minutes, and the absorbance at 500 nm was measured by spectrophotometry to quantify the lipid droplet content.

RNA extraction, cDNA reverse transcription and quantitative PCR (qPCR)

Total RNA was extracted from tissues and cells using the RNA isolater Total RNA Extraction Reagent (Vazyme, China). The RNA quantity was determined using a spectrophotometer (Thermo, USA). The purified RNA obtained in the previous step was reverse transcribed using the HiScript II Q RT SuperMix for qPCR (+gDNA wiper) kit (Vazyme, China) according to the manufacturer's instructions. MiRNA was reverse transcribed using the ReverTra Ace qPCR RT kit (Toyobo, Japan). qPCR was performed using the ChamQ Universal SYBR qPCR Master Mix (Vazyme, China) and the LightCycler 96 qPCR system (Roche, Basel, Switzerland). GAPDH and β-actin were used as internal controls for mRNA, and U6 was used as an internal control for miRNA. All experiments were performed with at least three biological replicates. The relative

quantification of genes was calculated using the $2^{-\Delta\Delta Ct}$ method. Specific primers, mimics, and inhibitors for BuLge-LoopTM miRNA qPCR were designed by RiboBio (RiboBio, China). The primer sequences are listed in Supplementary Table S1.

Vector construction and siRNA oligonucleotide synthesis

The CDS and 3′UTR sequences of the SESN1 gene were downloaded from the NCBI database (https://www.ncbi.nlm.nih.gov/). Using the laboratory-preserved expression vectors pcDNA3.1 and psiCHECK2, the SESN1 overexpression vector pcDNA3.1-SESN1 was constructed, along with the wild-type (**SESN1-3′UTR-WT**) and mutant (**SESN1-3′UTR-MUT**) vectors targeting miR-200b-3p, and the wild-type (**circADGRF5-WT**) and mutant (**circADGRF5-MUT**) vectors. The pCD25 expression vector, purchased from GENESEED (China), was used to construct the circADGRF5 expression vector pCD25-circADGRF5. The siRNA oligonucleotides for SESN1 (**si-SESN1**), negative control siRNA (**si-NC**), miR-200b-3p mimic, miR-200b-3p inhibitor, and their corresponding negative controls (mimic NC and inhibitor NC) were designed and synthesized by RiboBio.

Cell transfection

Cells were transfected using Lipofectamine 3000 (Invitrogen, USA) according to the manufacturer's instructions. Preadipocytes and DF-1 cells were seeded into 6-well plates and cultured until they reached 70-80 % confluence. Plasmids were transfected into the cells as required for the experiments. The transfection complexes were prepared in Opti-MEM (Gibco, USA) and added to the cells according to the Lipofectamine 3000 protocol. Six hours after transfection, the medium was replaced with fresh complete medium.

CCK-8, EdU assay and flow cytometry

CCK-8 Assay:Cell viability was measured using the CCK-8 kit (Vazyme, China). According to the manufacturer's instructions, 10 μL of CCK-8 solution was added to each well of a 96-well plate 2 hours before the measurement. The cell plates were then incubated at 37°C in a 5 % CO2 incubator. Cell viability of preadipocytes cultured in the 96-well plates was detected every 12 hours at a wavelength of 450 nm using a fluorescence microplate reader (BD BioTek, Winooski, USA).

EdU Assay:Cells were seeded into 24-well plates for culture. After 48 hours of transfection, the cells were fixed and incubated with the Cell-Light EdU Apollo 567 in vitro kit (RiboBio, China) according to the manufacturer's instructions. Images were captured using a fluorescence microscope (Olympus, Japan). All experiments were performed in triplicate.

Flow Cytometry:Preadipocytes seeded in 6-well plates were transfected at a concentration of 70 % (overexpression) and 40 % (knockdown). When the cells reached 90 %-100 % confluence, they were processed by first washing with PBS, followed by trypsin digestion. The digestion was stopped with complete medium to obtain a cell pellet. The cells were then resuspended in 70 % ethanol and fixed at 4°C. Cell cycle analysis was performed using a BD Accuri C6 flow cytometer (BD Biosciences, California, USA).

Cellular triglyceride (TG) measurement

Preadipocytes were washed twice with PBS and lysed using lysis buffer (Applygen, Beijing, China). The cell lysates were then incubated at 70°C for 10 minutes and centrifuged at 2000 rpm for 5 minutes at room temperature. Intracellular triglyceride (**TG**) levels were measured using a Cellular Triglyceride Content Assay Kit (Solarbio, China) according to the manufacturer's instructions.

Target gene prediction and dual luciferase reporter assay

The target genes of miRNAs were predicted using the bioinformatics tools miRDB and RNAhybrid (Chen et al., 2020; Krüger et al., 2006). The miRNA target validation experiments were conducted in DF-1 cells (Himly et al., 1998). Wild-type or mutant dual-luciferase reporter vectors were co-transfected with miR-200-3p mimics or NC mimics into DF-1 cells. The co-transfection was performed in 24-well plates using Lipofectamine 3000 reagent (Invitrogen, California, USA).

Gene function analysis

To elucidate the functions of the genes and further understand the biological connections of the regulated genes, we applied the ClusterProfiler package (Yu et al., 2012) for Gene Ontology (**GO**) term and Kyoto Encyclopedia of Genes and Genomes (**KEGG**) pathway analyses. Novel, high-quality visualizations of the data were created using the ggplot2 package in R (Maag JLV, 2018). Additionally, GO terms and KEGG pathways with a calibrated p (q) value < 0.05 were considered significantly enriched.

Identification of circular RNA

The cDNA and gDNA extracted from the abdominal fat tissue of Gushi chickens were used as templates for PCR amplification with forward and reverse primers specific to circADGRF5. The PCR products were subjected to gel electrophoresis, recovered, and subsequently sent to Beijing Tsingke Biotech Co., Ltd. for sequencing. The sequencing results were aligned with the junction sequence of circADGRF5 for comparative analysis. RNA samples isolated from the abdominal fat tissue of Gushi chickens underwent RNase R digestion following the protocol provided in the Ribonuclease R Kit (Guangzhou GENESEED). The cDNA from both the control group and the treatment group was then used as a template for qPCR to quantitatively analyze the expression levels and stability of circADGRF5. Refer to our previous method for details (Yuan et al., 2022).

Statistical analysis

Quantitative expression data from qRT-PCR were statistically analyzed using GraphPad Prism 8.0 software (GraphPad Software, USA). A t-test was performed to assess statistical differences in the data (*$p<$ 0.05, **$p<$ 0.01). Intergroup comparisons were analyzed using alphabetical superscript notation according to the following conventions: groups sharing identical letters (e.g., a,a) demonstrate statistically insignificant differences ($p>0.05$); those with distinct letter designations (e.g., a,b) exhibit statistically significant divergence ($p<0.05$); while groups marked with shared letter combinations (e.g., a,b) indicate partial significance overlaps with specific subgroups through multiple comparison analyses. The data are presented as the mean ± standard deviation (SEM) of at least three biological replicates.

Results

miR-200b-3p promotes proliferation and inhibits differentiation of preadipocytes

To investigate the effect of miR-200b-3p on chicken preadipocytes, this study first performed Oil Red O staining and image collection on primary preadipocytes of Gushi chickens at different stages of induced differentiation. Images were collected at six time points: 0d (start of induction when preadipocytes reached 80 % confluence), 1d, 2d, 3d, 4d, and 5d (Supplementary Fig. S1A). The results showed that the number of lipid droplets in adipocytes increased over the differentiation period. The expression levels of miR-200b-3p were validated by qRT-PCR at different stages of abdominal fat deposition (6 weeks, 14 weeks, 22

weeks, and 30 weeks) in Gushi chickens. The findings revealed differential expression of miR-200b-3p across these stages, with the highest expression observed at 6 weeks (Fig. 1A). Subsequently, the relative expression of miR-200b-3p in different tissues of 6-week-old Gushi chickens was analyzed, indicating high expression in abdominal fat tissue (Fig. 1B). Additionally, the changes in miR-200b-3p expression at different stages of induced differentiation were examined (Fig. 1C). The results demonstrated a significant downtrend in the first three days of differentiation compared to 0d, followed by an increase in expression in the later stages of induction. Collectively, the dynamic expression of miR-200b-3p at different stages and in different tissues suggests its potential involvement in the development of abdominal fat. Therefore, this study further validates its function at the cellular level.

During the proliferation phase of preadipocytes, miR-200b-3p mimic, mimic NC, miR-200b-3p inhibitor, and inhibitor NC were transfected into preadipocytes. Compared with the control group, the expression level of miR-200b-3p mimic was significantly increased in the overexpression group (Fig. 1D). In contrast, the expression level of miR-200b-3p was significantly decreased after transfection with the miR-200b-3p inhibitor compared to the control group (Fig. 1E). To validate the role of miR-200b-3p in the proliferation of preadipocytes, we measured the expression changes of proliferation-related marker genes using qRT-PCR. Cell proliferation activity was assessed with the CCK-8 assay, cell proliferation was quantified using the EdU assay, and the cell cycle was analyzed by flow cytometry. The results showed that after overexpressing miR-200b-3p, the expression level of the *P21* gene was significantly decreased, while the expression levels of *CDK1* and *CCNB2* were significantly increased compared to the control group (Fig. 1F). In contrast, after inhibiting miR-200b-3p, there was no significant change in the expression level of the P21 gene, but the expression levels of *CDK1, PCNA*, and *CCND1* were significantly decreased (Fig. 1G). The CCK-8 assay results indicated that cell viability was significantly increased at 12h, 24h, 36h, and 48h after overexpressing miR-200b-3p compared to the control group (Fig. 1H). Conversely, cell viability was significantly decreased at 12h, 24h, 36h, and 48h after inhibiting miR-200b-3p compared to the control group (Fig. 1I). The EdU assay results showed a significant increase in cell proliferation after transfection with the miR-200b-3p mimic (Fig 1J, L), whereas cell proliferation was significantly reduced after transfection with the miR-200b-3p inhibitor (Fig 1K, M). Flow cytometry analysis of the cell cycle revealed a significant increase in the proportion of S-phase cells after miR-200b-3p overexpression, with no significant changes in the G0/G1 and G2/M phases ($P > 0.05$) (Fig. 1N). In contrast, inhibition of miR-200b-3p resulted in no significant changes in the proportions of S-phase, G0/G1, and G2/M phase cells (Fig. 1O).

Furthermore, we examined the expression changes of differentiation-related marker genes using qRT-PCR, as well as the differentiation status of preadipocytes through Oil Red O staining and TG content measurement. The results indicated that overexpression of miR-200b-3p significantly decreased the expression levels of the differentiation marker genes *PPARγ, FABP4*, and *FABP5* (Fig. 1P), while inhibition of miR-200b-3p significantly increased the expression levels of the differentiation marker genes *C/EBPα, FABP4*, and *FABP5* (Fig. 1Q). Oil Red O staining revealed that overexpression of miR-200b-3p significantly reduced the number of lipid droplets in preadipocytes (Fig 1R, T), whereas inhibition of miR-200b-3p significantly increased the number of lipid droplets in preadipocytes (Fig 1S, U). The TG content measurement showed that the TG content in adipocytes was significantly decreased after transfection with miR-200b-3p mimic compared to the control group (Fig. 1V), while it was significantly increased in the miR-200b-3p inhibitor group (Fig. 1W). Collectively, these findings suggest that miR-200b-3p exhibits temporal expression during abdominal fat development in Gushi chickens, promoting preadipocyte proliferation and inhibiting preadipocyte differentiation in the abdominal region.

Screening and identification of miR-200b-3p target genes

To further investigate the molecular regulatory mechanisms of miR-200b-3p, we utilized the online tools miRDB and TargetScan to predict potential target genes of miR-200b-3p. A total of 1,223 potential target genes were identified. Gene Ontology (GO) (Fig. 2A) and Kyoto Encyclopedia of Genes and Genomes (KEGG) (Fig. 2B) functional enrichment analyses were performed on these potential target genes. The GO terms significantly enriched ($P < 0.05$) included protein amino acid complex, enzyme activity, amino acid transport, glycerolipid metabolic process, insulin receptor signaling pathway, and negative regulation of adipocyte differentiation. The KEGG pathways significantly enriched ($P < 0.05$) included the TGF-β signaling pathway, MAPK signaling pathway, insulin signaling pathway, adipocytokine signaling pathway, and steroid biosynthesis. Additionally, pathways related to fatty acid elongation, fatty acid metabolism, amino acid biosynthesis, and the PPAR signaling pathway were also enriched.

Combining our previous sequencing data for miRNA-mRNA correlation analysis and the prediction of miR-200b-3p potential target genes, we found that the pathway involving *SESN1* is closely related to lipid metabolism. Using bioinformatics prediction tools miRDB and RNAhybrid, we identified the predicted interaction between miR-200b-3p and its target gene *SESN1* (Fig. 2C-D). To further validate their targeting relationship, we constructed SESN1-3′UTR-WT and SESN1-3′UTR-MUT vectors for subsequent dual-luciferase reporter assays (Fig. 2E). After co-transfecting DF-1 cells with miR-200b-3p mimic and either the wild-type or mutant psiCHECK2-SESN1-3′UTR vectors for 48 hours, miR-200b-3p was found to significantly inhibit the luciferase activity of the wild-type vector ($P < 0.01$), while there was no significant inhibitory effect when co-transfected with the mutant vector (Fig. 2F). To further validate the targeting interaction between miR-200b-3p and the *SESN1* gene, we overexpressed and inhibited miR-200b-3p in preadipocytes, respectively, and detected changes in *SESN1* mRNA levels using qRT-PCR. Overexpression of miR-200b-3p in preadipocytes significantly suppressed *SESN1* gene expression ($P < 0.05$) (Fig. 2G). Conversely, inhibition of miR-200b-3p significantly promoted *SESN1* gene expression ($P < 0.01$) (Fig. 2H). These results indicate that there is a targeting interaction between miR-200b-3p and the *SESN1* gene.

SESN1 inhibits preadipocyte proliferation and promotes their differentiation

To investigate the role of *SESN1* in the proliferation and differentiation of chicken preadipocytes, we first examined the expression changes of *SESN1* in different tissues of 6-week-old Gushi chickens and at various time points during the induced differentiation of preadipocytes. This was done to better understand the expression patterns of *SESN1*. The results showed that *SESN1* was highly expressed in the abdominal fat of Gushi chickens (Fig. 3A) and exhibited a gradually increasing trend at different time points during preadipocyte differentiation (Fig. 3B). The dynamic expression patterns of *SESN1* in different tissues and differentiation stages suggest its potential involvement in fat development. Therefore, we proceeded to validate its function at the cellular level.

Firstly, when preadipocytes reached 80 % confluence, we transfected the overexpression vector pcDNA3.1-SESN1 and the control vector pcDNA3.1, as well as the interference fragment si-SESN1 and the control si-NC into the preadipocytes. Compared with the control group transfected with pcDNA3.1, the expression of *SESN1* significantly increased in the overexpression group (Fig. 3C). Conversely, the expression of *SESN1* significantly decreased after transfection with the interference fragment si-SESN1 (Fig. 3D). We validated the role of *SESN1* in the proliferation of preadipocytes using qRT-PCR, CCK-8, EdU, and cell cycle assays. The results showed that overexpression of *SESN1* significantly increased the expression of the *P21* gene and decreased the expression levels of *CDK1, PCNA, CCND1*, and *CCNB2* compared to the

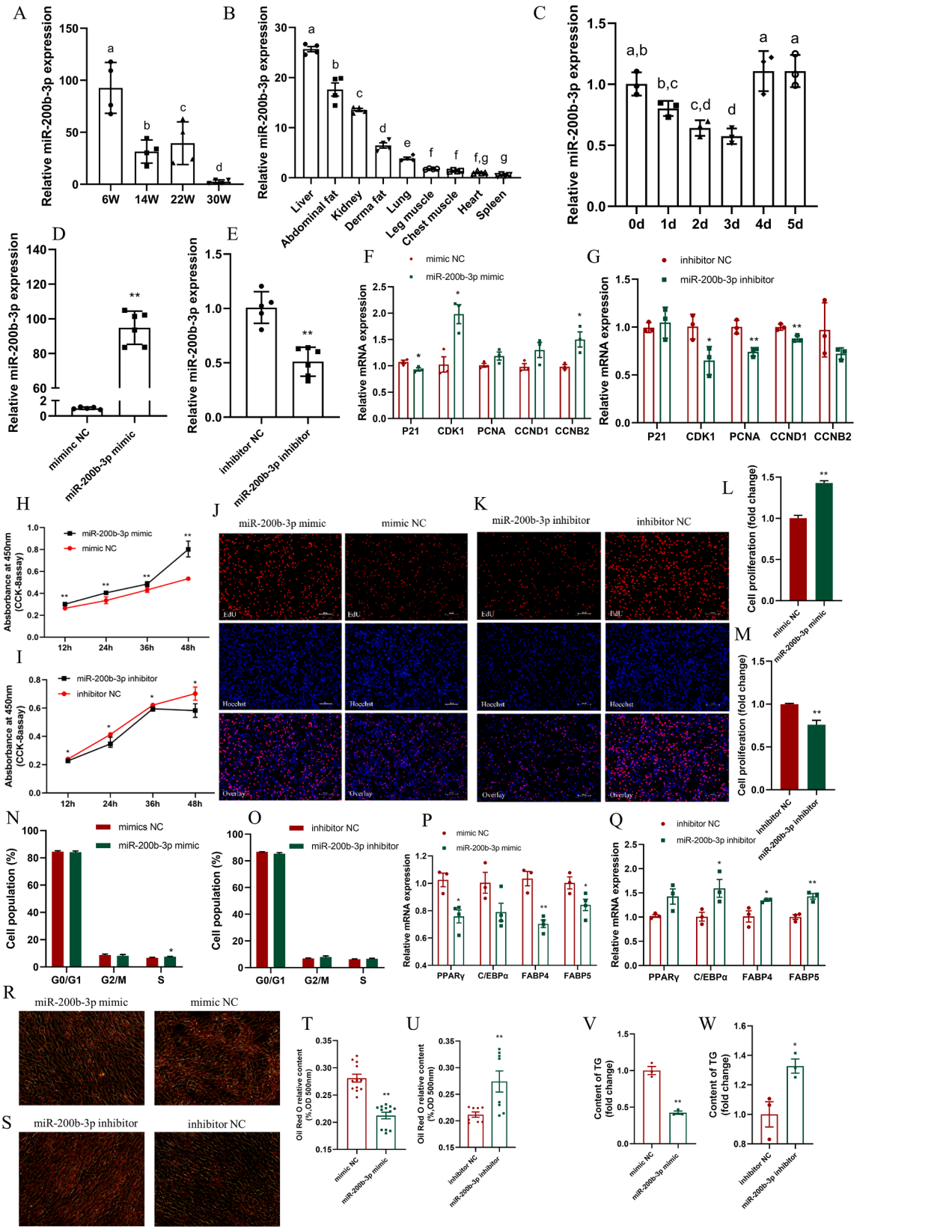

(caption on next page)

Fig. 1. miR-200b-3p promotes the proliferation of preadipocytes and inhibits their differentiation. (A) Relative expression of miR-200b-3p in abdominal adipose tissue of Gushi chickens at different periods. (B) Relative expression of miR-200b-3p in different tissues of Gushi chickens at 6 weeks of age. (C) Relative expression of miR-200b-3p in preadipocytes at different differentiation time points. (D) Detection of overexpression efficiency of miR-200b-3p. (E) Detection of inhibitory efficiency of miR-200b-3p. (F) Effects of overexpression of miR-200b-3p on proliferative marker genes. (G) Effects of inhibition of miR-200b-3p on proliferative marker genes. (H) Effects of overexpression of miR-200b-3p on the proliferation activity of preadipocyte. (I) The effect of inhibition miR-200b-3p on the proliferation activity of preadipocyte. (J) EdU detected the effect of miR-200b-3p expression on the number of preadipocyte proliferation. (K) The effect of EdU detection on the proliferation number of preadipocytes after inhibition of miR-200b-3p. (L) The proportion of EdU positive cells. (M) Statistics of the proportion of EdU positive cells. (N) Effects of overexpression of miR-200b-3p on the cell cycle of preadipocyte. (O) The effect of interfering with miR-200b-3p on the cell cycle of preadipocyte. (P) Effect of overexpression of miR-200b-3p on differentiation marker genes. (Q) Effect of inhibition of miR-200b-3p on differentiation marker genes. (R) Results of oil red O staining after overexpression of miR-200b-3p. (S) Results of oil red O staining after inhibition of miR-200b-3p. (T-U) Analysis of oil red O content (OD value read at 500 nm). (V) Detection results of TG content after overexpression of miR-200b-3p. (W) Detection results of TG content after inhibition of miR-200b-3p. All experiments were performed in triplicate, and the data are expressed as the mean ±S.E.M. (* $p<0.05$; ** $p<0.01$). Statistical comparisons between groups were denoted using alphabetical superscripts: identical lettersindicate no significant difference ($p>0.05$), distinct letters represent significant differences ($p<0.05$).

control group (Fig. 3E). In contrast, inhibition of *SESN1* led to a significant decrease in the expression of the P21 gene and a significant increase in the expression of *CCND1*, while the expression levels of *CDK1, PCNA*, and *CCNB2* did not show significant changes (Fig. 3F). The cell cycle results indicated that overexpression of *SESN1* resulted in no significant changes in the G0/G1 and G2/M phases, but a significant reduction in the S phase cells compared to the control group (Fig. 3G). Conversely, inhibition of *SESN1* significantly decreased the G0/G1 phase, significantly increased the G2/M phase, and significantly increased the S phase cells (Fig. 3H). The EdU assay results indicated that cell proliferation was significantly reduced after transfection with pcDNA3.1-SESN1 (Fig. 3I), whereas cell proliferation significantly increased after transfection with si-SESN1 (Fig. 3J). The CCK-8 assay results showed that cell viability significantly decreased at 24h, 36h, and 48h after overexpression of *SESN1* compared to the control group (Fig. 3K). In contrast, cell viability significantly increased at 24h and 36h after inhibition of *SESN1* expression (Fig. 3L).

We further investigated the impact of *SESN1* on the differentiation of preadipocytes. By overexpressing and inhibiting *SESN1* in preadipocytes, we examined the expression of differentiation marker genes, performed Oil Red O staining, and measured TG content to assess the differentiation status of preadipocytes. The results showed that overexpression of *SESN1* significantly increased the expression levels of the differentiation marker genes *PPARγ* and *C/EBPα*, while the expression levels of *LPL, FABP4*, and *FABP5* showed no significant changes (Fig. 3O). In contrast, inhibition of *SESN1* significantly decreased the expression levels of the differentiation marker genes *PPARγ, LPL*, and *FABP4*, with no significant changes in the expression levels of *C/EBPα* and *FABP5* (Fig. 3P). Oil Red O staining results revealed that overexpression of *SESN1* significantly increased the number of lipid droplets in preadipocytes (Supplementary Fig.s S1B), whereas inhibition of *SESN1* significantly reduced the number of lipid droplets in preadipocytes (Supplementary Fig.s S1C). TG content measurements showed that, compared to the control group, TG content in adipocytes significantly increased after *SESN1* overexpression (Fig. 3M), while TG content significantly decreased in the si-SESN1 transfection group (Fig. 3N).

To further elucidate whether miR-200b-3p regulates preadipocyte proliferation and differentiation through its targeting of the *SESN1* gene, we co-transfected miR-200b-3p mimic with pcDNA3.1-SESN1, miR-200b-3p mimic with pcDNA3.1, and mimic NC with pcDNA3.1 into preadipocytes. The results showed that the expression of *P21* was significantly decreased in the miR-200b-3p mimic + pcDNA3.1 group, whereas the expression of *P21* was restored in the miR-200b-3p mimic + pcDNA3.1-SESN1 group, indicating that the inhibitory effect was weakened. Similarly, the expression of other proliferation marker genes *PCNA, CCND1*, and *CCNB2* was significantly inhibited in the miR-200b-3p mimic + pcDNA3.1-SESN1 group compared to the miR-200b-3p mimic + pcDNA3.1 group (Fig. 3Q). The expression levels of differentiation marker genes *PPARγ, C/EBPα, FABP4*, and *FABP5* were significantly higher in the miR-200b-3p mimic + pcDNA3.1-SESN1 group than in the miR-200b-3p mimic + pcDNA3.1 group, but still lower than those in the mimic NC + pcDNA3.1 group (Fig. 3R). Additionally, we further demonstrated that miR-200b-3p regulates preadipocyte proliferation and differentiation through its targeting of the SESN1 gene by co-transfecting the cells and performing CCK-8 assays and cell cycle analysis. The CCK-8 assay results indicated that the cell proliferation activity in the miR-200b-3p mimic + pcDNA3.1-SESN1 group was significantly higher than that in the control group, but lower than that in the miR-200b-3p overexpression group (Supplementary Fig. S1D). Cell cycle analysis revealed that the number of G0/G1 phase cells in the miR-200b-3p mimic + pcDNA3.1-SESN1 group was significantly higher than that in the miR-200b-3p overexpression group, while the number of G2/M phase cells was significantly lower than that in the miR-200b-3p overexpression group. The number of S phase cells in the miR-200b-3p overexpression group was significantly higher than that in the other two groups, but the number of S phase cells in the miR-200b-3p mimic + pcDNA3.1-SESN1 group was lower than that in the control group (Supplementary Fig. S1E). These results suggest that miR-200b-3p can mitigate the inhibitory effect of *SESN1* on cell proliferation activity.

In summary, our results indicate that *SESN1* exhibits temporal expression during the process of adipocyte differentiation, where it inhibits preadipocyte proliferation and promotes differentiation. This effect is directly regulated by the targeting action of miR-200b-3p.

circADGRF5 Competitively Binds miR-200b-3p to regulate SESN1 expression

We obtained the gene information of *ADGRF5* and the circular RNA (circRNA) formation mechanism from the NCBI database. Combined with circRNA sequencing, we predicted that circADGRF5 is formed by the self-circularization of *ADGRF5*, with a full length of 590 nt. We designed forward and reverse primers for circADGRF5 and performed PCR amplification using mixed gDNA and cDNA samples from the abdominal fat tissues of Gushi chickens at different ages. The results showed that both primer pairs successfully amplified the target product from cDNA; the forward primers could also amplify the target fragment using gDNA as a template, while the reverse primers could not amplify any bands from gDNA (Fig. 4A). Subsequently, Sanger sequencing of the fragments amplified with the reverse primers revealed the presence of the expected back-spliced junction sequence (Fig. 4B). We also used RNase R digestion to further verify circADGRF5, and qRT-PCR results indicated that circADGRF5 was resistant to RNase R digestion (Fig. 4C). These results collectively confirm that circADGRF5 is a stable and authentic circRNA.

Based on our previous sequencing data for miRNA-circRNA correlation analysis and the prediction results of potential circRNAs for miR-200b-3p (Jin et al., 2021), we constructed circADGRF5-WT and circADGRF5-MUT vectors to validate their targeting relationship (Fig. 4D). Subsequently, we transfected DF-1 cells with miR-200b-3p mimic or mimic NC, and circADGRF5-WT or circADGRF5-MUT. After 48 hours of co-transfection, the fluorescence values of each group were measured using a dual-luciferase reporter assay. The results showed that the fluorescence activity in the miR-200b-3p mimic + circADGRF5-WT

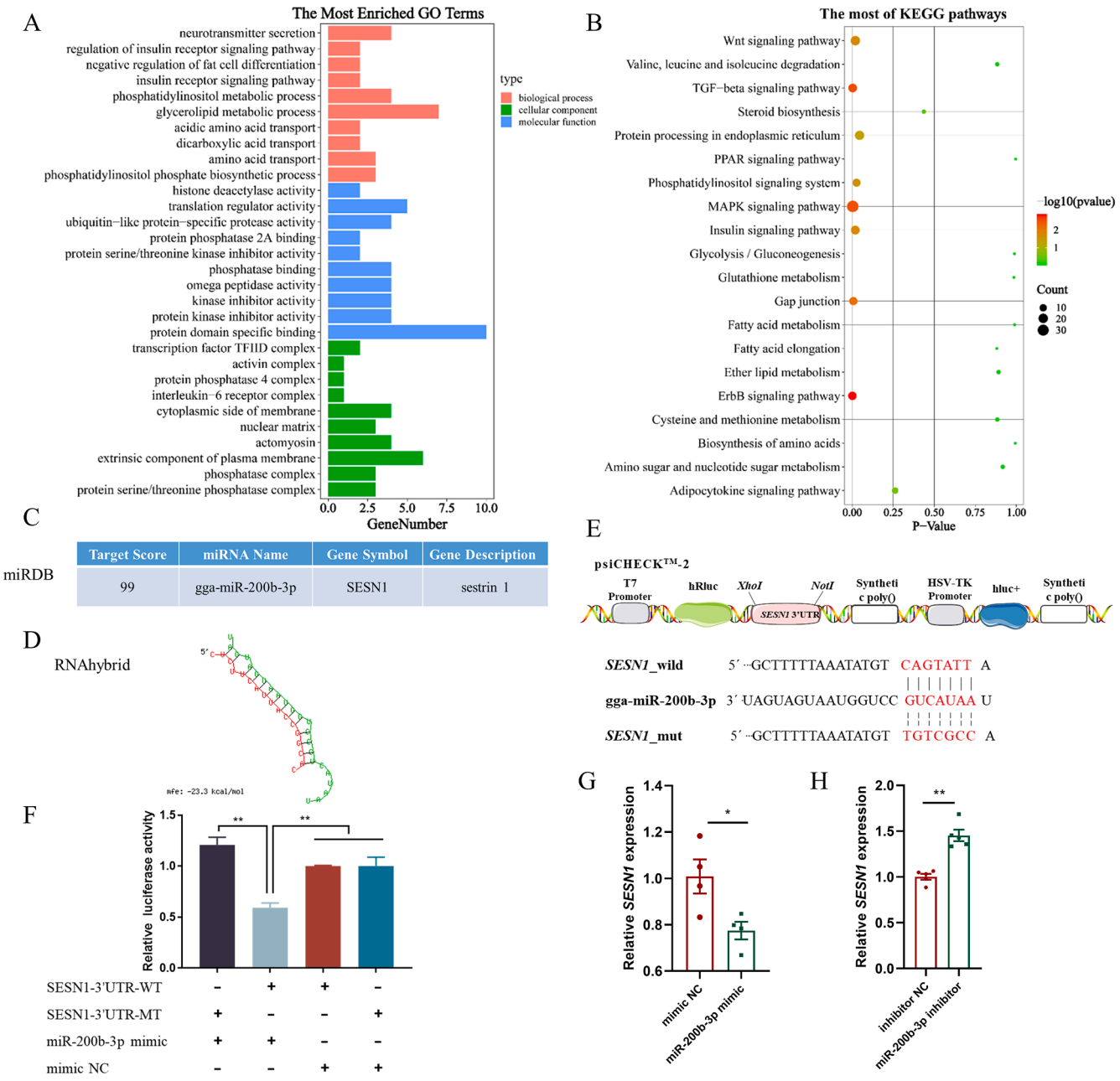

Fig. 2. Screening and Identification of Target Genes of miR-200b-3p. (A) The y-axis is the GO items at the next level of the three GO categories, and the x-axis is the number of genes annotated for that item. (B) The y-axis indicates the pathway name, the x-axis indicates the p-value, the size of the dots indicates the number of genes in the pathway, and the color of the dots corresponds to different -log10 (q-value) ranges. (C-D) *SESN1* was predicted to be a target of miR-200b-3p by miRDB and RNAhybrid. (E) Binding site of miR-200b-3p and the 3'UTR sequence of *SESN1* gene. (F) Validation of *SESN1* gene as miR-200b-3p target. (G-H) Effects of overexpression/inhibitory of miR-200b-3p on the relative expression of *SESN1*. All experiments were performed in triplicate, and the data are expressed as the mean ±S.E.M. (* $p<0.05$; ** $p<0.01$).

group was significantly lower than that in the mimic NC + circADGRF5-WT group ($P < 0.01$), and also significantly lower than that in the miR-200b-3p mimic + circADGRF5-MUT and mimic NC + circADGRF5-MUT groups ($P < 0.01$) (Fig. 4E). qRT-PCR results indicated that the expression level of circADGRF5 was significantly decreased or increased after overexpressing or inhibiting miR-200b-3p, respectively (Fig 4F-G). These findings suggest a targeting relationship between miR-200b-3p and circADGRF5.

We used pCD25 as the overexpression vector to construct a circADGRF5 overexpression plasmid, named pCD2-circADGRF5, with the empty pCD25 plasmid as the control. The constructed plasmids and the control were transfected into preadipocytes to verify the overexpression effect. The results showed that the overexpression plasmid significantly upregulated the expression of circADGRF5 (Fig. 4H). Next, we investigated whether circADGRF5 competitively binds miR-200b-3p to regulate *SESN1* expression through co-transfection recovery experiments. We co-transfected pCD2-circADGRF5 with miR-200b-3p mimic or mimic NC and found that circADGRF5 could indeed rescue the inhibitory effect of miR-200b-3p on *SESN1* expression (Fig. 4I). Additionally, we co-transfected pCD2-circADGRF5 or the control plasmid with miR-200b-3p inhibitor or inhibitor NC. The results showed that both pCD2-circADGRF5 and miR-200b-3p inhibitor groups upregulated *SESN1* expression, but there was no significant difference between the pCD2-circADGRF5 + miR-200b-3p inhibitor group and the pCD25 + miR-

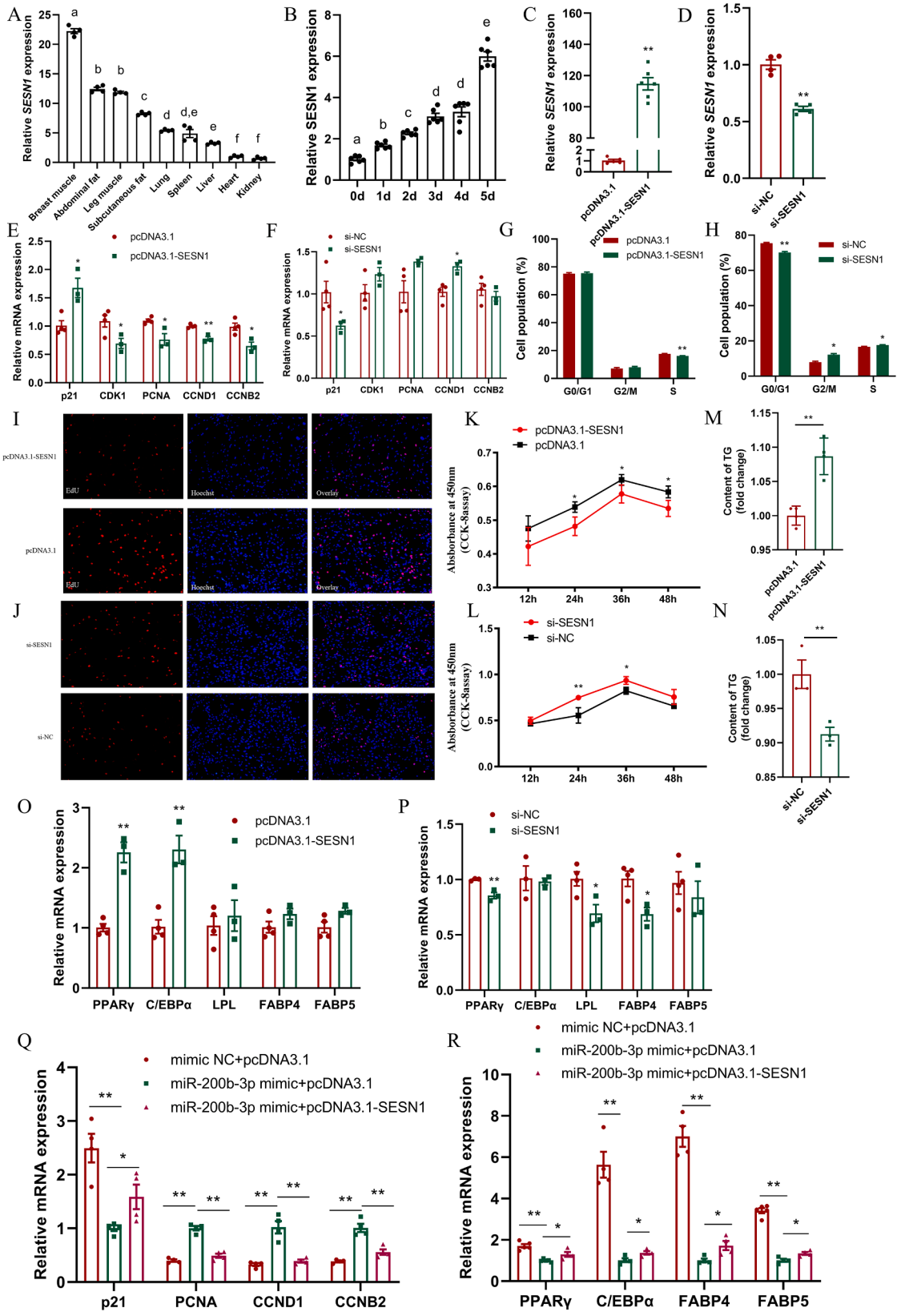

(caption on next page)

Fig. 3. *SESN1* inhibits the proliferation of preadipocytes and promotes their differentiation. (A) Relative expression of *SESN1* in different tissues of Gushi chickens at 6 weeks of age. (B) Relative expression of *SESN1* in preadipocytes at different differentiation time points. (C) Detection of overexpression efficiency of *SESN1*. (D) Detection of interference efficiency of *SESN1*. (E) Effects of overexpression of SESN1on proliferative marker genes. (F) Effects of interference of SESN1on proliferative marker genes. (G) Effects of overexpression of *SESN1* on the cell cycle of preadipocyte. (H) The effect of interfering with *SESN1* on the cell cycle of preadipocyte. (I) The effect of overexpression of *SESN1* on the proliferation of preadipocyte detected by EdU. (J) Effects of EdU detection on the proliferation of preadipocyte by interfering with SESN1. (K) Effects of overexpression of *SESN1* on the proliferation activity of preadipocyte. (L) The effect of interfering *SESN1*on the proliferation activity of preadipocyte. (M) Detection results of TG content after overexpression of *SESN1*. (N) Detection results of TG content after interference of *SESN1*. (O) Effects of overexpression of *SESN1* on differentiation marker genes. (P) The effect of interfering with *SESN1* on differentiation marker genes. (Q) The expression of proliferative marker genes changed after co-transfection. (R) Changes in the expressionof differentiation marker genes after co-transfection. All experiments were performed in triplicate, and the data are expressed as the mean ±S.E.M. (* $p<0.05$; ** $p<0.01$). Statistical comparisons between groups were denoted using alphabetical superscripts: identical lettersindicate no significant difference ($p>0.05$), distinct letters represent significant differences ($p<0.05$).

200b-3p inhibitor group (Fig. 4J). This indicates that circADGRF5 exerts its regulatory effect on *SESN1* by binding to miR-200b-3p. However, when miR-200b-3p is inhibited, the increase in *SESN1* expression is due to the effect of the miR-200b-3p inhibitor, and thus overexpression of circADGRF5 loses its regulatory effect on *SESN1*.

Similarly, to further confirm that circADGRF5 regulates *SESN1* expression by competitively binding to miR-200b-3p, we co-transfected circADGRF5-WT, miR-200b-3p mimic, and SESN1-3′UTR-WT into DF-1 cells. After 48 hours, a dual-luciferase reporter assay was performed to measure the fluorescence values. The results showed that the fluorescence value in the miR-200b-3p mimic + SESN1-3′UTR-WT group was significantly lower than that in the miR-200b-3p mimic group, while the presence of circADGRF5-WT resulted in a partial recovery of the fluorescence value (Fig. 4K). This suggests that circADGRF5 can mitigate the inhibitory effect of miR-200b-3p on *SESN1*.

Discussion

Excessive accumulation of abdominal fat in chickens has become an unavoidable issue in modern animal husbandry, and such fat accumulation can also impact human health. It is well-known that fat deposition in chickens is a highly complex biological process regulated by various pathways, transcription factors, and genes (Moreira et al., 2018; Davoli et al.,2016). To elucidate the process and regulatory mechanisms of abdominal fat deposition in chickens post-hatch, we previously conducted high-throughput sequencing of abdominal fat tissues in Gushi chickens at 6, 14, 22, and 30 weeks of age. This comprehensive evaluation revealed the expression profiles of miRNA, circRNA, lncRNA, and mRNA during the development of abdominal fat in Gushi chickens (Jin et al., 2021; Zhai et al., 2023). Through integrated analysis of the sequencing data, we constructed an interaction regulatory network related to abdominal fat deposition in Gushi chickens. Our findings revealed that miR-200b-3p exhibited significant differential expression at various stages of abdominal fat development, and further identified the interaction between circADGRF5/miR-200b-3p/*SESN1*, which is involved in the development or deposition of abdominal fat in chickens.

Abdominal fat deposition involves an increase in the number and hypertrophy of adipocytes. Numerous studies have demonstrated the critical role of miRNA in the growth and development of adipocytes (Huang et al.,2010; Wang et al., 2008; Sun et al., 2009; Huang et al., 2012). In this study, we investigated the effects of miR-200b-3p on preadipocytes by transfecting preadipocytes with miR-200b-3p mimics and inhibitors. Several studies have shown that certain cell cycle-related genes are involved in the progression of the cell cycle, with *P21* being one of the key downstream genes in the p53 signaling pathway. *P21* can inhibit the activity of the cyclin-CDK complex and *PCNA*, inducing cell cycle arrest and senescence in response to DNA damage (Chen et al., 2008). Genes related to cell proliferation, such as *P21, PCNA, CDK1, CCND1*, and *CCNB2*, are commonly used to assess cell proliferation status (Chen et al., 2008). Our study found that miR-200b-3p could suppress the expression of *P21* while promoting the expression of other proliferation marker genes. Flow cytometry results indicated that miR-200b-3p facilitates the progression of cells through the S phase. Additionally, CCK-8 and EdU assays demonstrated that miR-200b-3p promotes the proliferation of preadipocytes. Therefore, the results of this study demonstrate that miR-200b-3p can promote the proliferation of preadipocytes. It is well-known that *PPARγ* and *C/EBPα* are the most important transcription factors for adipogenesis and can serve as markers of adipocyte differentiation (Jin et al., 2010; Marion et al., 2016). This study found that overexpression of miR-200b-3p significantly reduces the mRNA expression levels of *PPARγ* and *C/EBPα*. Additionally, Oil Red O staining and triglyceride content assays revealed that overexpression of miR-200b-3p decreases lipid droplet accumulation in adipocytes and significantly reduces intracellular triglyceride levels. Conversely, inhibiting miR-200b-3p produced opposite results. These findings collectively confirm that miR-200b-3p can inhibit the differentiation of preadipocytes.

An increasing number of studies indicate that miRNAs exert their regulatory functions by inhibiting or degrading downstream target genes, thereby modulating gene expression at the post-transcriptional level (Correia et al., 2019). Therefore, investigating the regulatory network between miRNAs and their target genes are of significant importance. In fact, miRNA-mediated regulation of gene expression is influenced by various factors, which may vary depending on the cellular or tissue environment (Bhaskaran et al., 2014). A notable characteristic of miRNAs is that a single miRNA can target multiple mRNAs, thereby regulating the expression of an entire set of proteins; conversely, a single mRNA can be targeted by multiple miRNAs (Wang et al., 2012; Gjorgjieva et al., 2019). To explore the post-transcriptional regulatory mechanism of miR-200b-3p, we performed a miRNA-mRNA association analysis based on our previous sequencing data, identifying numerous genes with potential miR-200b-3p binding sites (Chen et al., 2019). Using online tools such as miRDB and TargetScan, we predicted 1,223 potential target genes of miR-200b-3p and conducted GO and KEGG functional enrichment analyses on these predicted targets. The results revealed significant enrichment in pathways related to lipid metabolism, such as amino acid transport, fatty acid metabolism, triglyceride metabolic process, insulin receptor signaling pathway, steroid biosynthesis, negative regulation of adipocyte differentiation, and the PPAR signaling pathway. Previous research has shown that overexpression of miR-200b can reduce the expression levels of downstream genes of *KLF4* in 3T3-L1 cells, such as *PPARγ* and *C/EBPα* (Shen et al., 2018). Hence, we hypothesize that miR-200b-3p may interact with its corresponding target genes, collectively participating in the processes of adipogenesis or fat deposition. Integrating the results of the enrichment analysis with the miRNA-mRNA association analysis, we identified the miR-200b-3p/*SESN1* axis as a key focus for further validation. A recent study discovered that *SESN1*, an important member of the Sestrin family, plays a crucial role in lipid metabolism. Mice lacking Sestrin1 exhibit rapid loss of white adipose tissue when dietary leucine is reduced (Cangelosi et al., 2022). Additionally, *SESN2* ablation exacerbates lipodystrophy, glucose intolerance, and insulin resistance, suggesting that this protein family plays a homeostatic role in controlling glucose and lipid metabolism (Lee et al., 2012). Overexpression of *SESN*1 induces the expression of fatty acid oxidation-related genes in mouse hepatocytes, such as *PDK4* and *PPARα* (Geng et al., 2022). Furthermore, a prior study indicated that miR-200c inhibits cholangiocyte proliferation and neuroendocrine-like activation by targeting *SESN1* and suppressing the

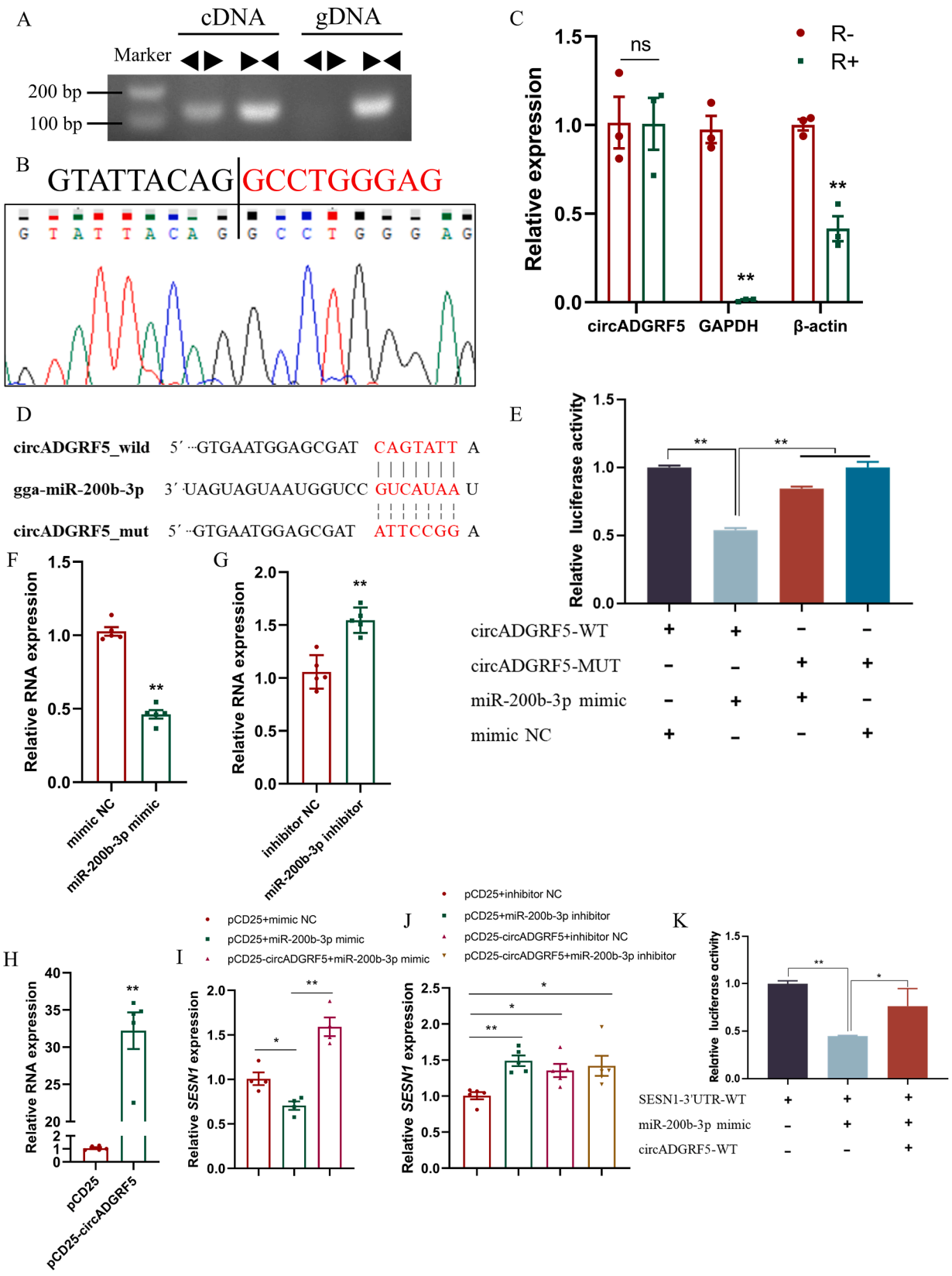

Fig. 4. circADGRF5 competitively binds to miR-200b-3p to regulate the expression of *SESN1*. (A) PCR electrophoresis of forward primers and backward primers. (B) Sanger sequencing to verify the joint sequence. (C) qRT-PCR results after RNase R enzyme treatment. (D) Analysis of the binding sites of miR-200b-3p and circADGRF5. (E) Dual luciferase reporting assay to verify the targeting relationship. (F) The expression of circADGRF5 after overexpression of miR-200b-3p. (G) The expression of circADGRF5 after the inhibition of miR-200b-3p. (H) Verification results of circADGRF5 overexpression. (I) Expression changes of SESN1 after co-transfection of overexpressed circADGRF5 plasmid with miR-200b-3p mimic. (J) Expression changes of *SESN1* after co-transfection with overexpressed circADGRF5 plasmid and miR-200b-3p inhibitor. (K) circADGRF5 competitively binds to miR-200b-3p to reduce inhibition of *SESN1*. All experiments were performed in triplicate, and the data are expressed as the mean ±S.E.M. (* $p<0.05$; ** $p<0.01$).

IL-6/AKT feedback loop (Song et al., 2022). These findings suggest that *SESN1* may play a pivotal role in the process of adipogenesis or fat deposition. Our study employed dual-luciferase reporter assays and qRT-PCR experiments to confirm the targeting relationship between miR-200b-3p and *SESN1*. Consequently, the regulatory effect of miR-200b-3p on preadipocytes is likely achieved through direct targeting of *SESN1*.

Sestrin 1 (***SESN1***), as a stress-induced protein, is an indispensable gene in vertebrates (Peeters et al., 2006). *SESN1* is extensively involved in various biological functions in animals, including cell growth, inflammation, fat accumulation, and tumor suppression (Zhang et al., 2022; Cordani et al., 2018). Previous research has demonstrated that *SESN1* can directly target miR-16-5p to promote the differentiation of chicken myoblasts (Cai et al., 2018). Silencing *SESN1* can counteract the overexpression effects of the transcription factor Forkhead Box Protein 1 (***FOXP1***), thereby inhibiting inflammation and lipid accumulation in oxidized low-density lipoprotein-treated RAW264.7 cells (Gao et al., 2022). Functional prediction analysis of *SESN1* (https://www.kegg.jp/kegg/pathway.html) revealed that it is a key gene in the p53 signaling pathway, with functions related to the cell cycle and DNA repair, consistent with previous findings where *SESN1* was enriched in cell cycle and apoptosis-related functions (Apostolidis et al., 2012). As early as 1994, *SESN1* was identified as a p53-responsive gene (Buckbinder et al., 1994). A recent study indicated that the inhibition of *SESN1* might be associated with the upregulation of Ras-induced reactive oxygen species (**ROS**) and is involved in regulating cellular activities, including proliferation, survival, and differentiation (Zamkova et al., 2013). In chickens, *SESN1* can regulate the p53 signaling pathway via a feedback mechanism, promoting myoblast proliferation and inhibiting apoptosis (Cai et al., 2018). Our results showed high expression of *SESN1* in the muscle and fat tissues of Gushi chickens, corroborating its role in promoting myoblast differentiation. Monitoring *SESN1* expression levels across different tissues and at various stages of differentiation suggests that *SESN1* might be involved in the proliferation and differentiation of preadipocytes. Overexpression of *SESN1* in preadipocytes resulted in a significant increase in the expression of the cell cycle inhibitory gene *P21*, while the expression levels of other proliferation marker genes such as *CDK1, PCNA, CCND1*, and *CCNB2* were significantly decreased. Conversely, interfering with *SESN1* expression yielded opposite results. Flow cytometry results further supported our hypothesis, showing that *SESN1* inhibited the progression of the S phase. Additionally, CCK-8 results confirmed that *SESN1* suppressed the proliferative activity of preadipocytes, and EdU assay results indicated that overexpression of *SESN1* significantly reduced the number of proliferating preadipocytes. Thus, *SESN1* acts as a negative regulator of adipogenesis. Our study also examined the expression levels of mRNAs related to adipocyte differentiation and found that overexpression of *SESN1* significantly promoted the expression of differentiation transcription factors *PPARγ* and *C/EBPα*. This led to a substantial increase in the number of lipid droplets in preadipocytes and a significant elevation in triglyceride content within adipocytes. These findings demonstrate that *SESN1* can promote preadipocyte differentiation, consistent with its elevated expression levels during the differentiation period of preadipocytes.

Our experimental results have validated that *SESN1* is a direct target gene of miR-200b-3p. In this study, we found that *SESN1* expression is consistently upregulated during the differentiation of preadipocytes, while miR-200b-3p expression is consistently downregulated during the first 0-3 days of differentiation, showing a negative correlation with *SESN1* expression. Therefore, it is hypothesized that the effect of *SESN1* on preadipocytes may be regulated by miR-200b-3p. To test this hypothesis, we performed rescue experiments by co-transfecting miR-200b-3p mimics and *SESN1* overexpression plasmids into preadipocytes. The results showed that co-transfection of miR-200b-3p and *SESN1* reversed the proliferative effect of miR-200b-3p on preadipocytes and also reversed the inhibitory effect on the expression of differentiation marker genes *PPARγ, C/EBPα, FABP4*, and *FABP5*. These findings collectively indicate that the role of miR-200b-3p in chicken preadipocytes is primarily mediated through the suppression of *SESN1* expression, which leads to increased adipocyte proliferation and inhibition of differentiation, thereby enhancing abdominal fat deposition.

ADGRF5 is an important member of the G protein-coupled receptor (**GPCR**) family, which is a large and diverse family of integral membrane proteins capable of recognizing a wide variety of extracellular molecules and participating in most physiological processes (Zaidman et al., 2020; Bockaert et al., 1999). Research has shown that a significant member of the GPCR family, GPR116, serves as a receptor for soluble *FNDC4* (**sFNDC4**) in white adipose tissue, promoting insulin signaling and insulin-mediated glucose uptake in adipocytes (Georgiadi et al., 2021). This suggests that *ADGRF5* may play a role in adipogenesis. *ADGRF5* can form a circular RNA, circADGRF5, which was validated through junction sequence verification, Sanger sequencing, and RNase R digestion assays, confirming that circADGRF5 is a truly stable circular RNA. Increasing evidence indicates that a prominent feature of circRNAs is their role as miRNA sponges, regulating the functions of target genes through the ceRNA mechanism (Panda AC., 2018). Therefore, we integrated the previous circRNA-miRNA-mRNA joint analysis data from the abdominal fat tissues of Gushi chickens to predict miRNA binding sites on the circRNA sequence (Jin et al., 2021). The results indicated that the identified circRNAs have numerous potential miRNA binding sites, including a sequence in circADGRF5 that can target the seed sequence of miR-200b-3p. To verify this targeting relationship, we constructed circADGRF5-WT and circADGRF5-MUT dual-luciferase reporter vectors. The results showed that the fluorescence value of wild-type circADGRF5 co-transfected with miR-200b-3p was significantly reduced, indicating a direct targeting relationship. Studies have demonstrated that circBIRC6 is enriched in AGO2 protein complexes and directly interacts with miR-34a and miR-145 to inhibit the differentiation of human embryonic stem cells (Yu et al., 2017). Similarly, circHIPK2 functions as an endogenous sponge for miR-124, sequestering miR-124HG and inhibiting its activity, leading to increased expression of *SIGMAR1/OPRS1* in astrocytes (Huang et al., 2017). To explore whether circADGRF5 acts as a molecular sponge for miR-200b-3p, we performed rescue experiments by co-transfecting circADGRF5 and miR-200b-3p. The results showed that when circADGRF5 and miR-200b-3p were co-overexpressed, the inhibitory effect of miR-200b-3p on its target gene *SESN1* was significantly attenuated. Additionally, dual-luciferase reporter assays confirmed that wild-type circADGRF5 could significantly restore the fluorescence values when miR-200b-3p and SESN1-3′UTR-WT were co-expressed. In conclusion, our findings suggest that circADGRF5 can function as a molecular sponge for miR-200b-3p, alleviating its inhibitory effect on *SESN1*, thereby participating in the regulation of abdominal fat formation.

Conclusion

In this study, we investigated the biological functions of miR-200b-3p and *SESN1* in chicken preadipocytes, demonstrating that miR-200b-3p directly targets *SESN1* to regulate the proliferation and differentiation of these cells. We also identified a novel circular RNA, circADGRF5, which has a targeting relationship with miR-200b-3p. Our findings show that circADGRF5 regulates *SESN1* expression by competitively binding to miR-200b-3p, thereby influencing the proliferation and differentiation of preadipocytes. These insights provide a new understanding of the mechanisms underlying abdominal fat development in chickens and the post-transcriptional regulatory processes involved.

Author contributions

PY and HL: Validation, Visualization, Writing - original draft. **HZ and SF:** Data curation and Software. **YD, JJ and JS:** Validation and Data curation. **YZ, HL and GS:** Formal analysis, Investigation and

Methodology. **XL, YT and XK:** Conceptualization, Formal analysis, Supervision and Resources. **YZ and GL:** Conceptualization, Funding acquisition, Project administration, Writing - review & editing. All authors approved the final manuscript.

Declaration of competing interest

The authors of this study declare that they have no financial or non-financial conflicts of interest during the course of the research.

All data and findings presented in this study are original, and there are no external financial relationships or conflicts of interest that could have influenced the results.

If there are any further questions, please contact the corresponding author.

Acknowledgments

This work was supported by grants from Key Research Project of the Shennong Laboratory (SN01-2022–05), the National Natural Science Foundation of China (32072692), the National Key Research and Development Program of China (2023YFF1001100).

Disclosure statement

The authors have nothing to disclose.

Supplementary materials

Supplementary material associated with this article can be found, in the online version, at doi:10.1016/j.psj.2025.105068.

References

Ambros, V., 2004. The functions of animal microRNAs. Nature 431 (7006), 350–355.
Apostolidis, P.A., Lindsey, S., Miller, W.M., Papoutsakis, ET., 2012. Proposed megakaryocytic regulon of p53: the genes engaged to control cell cycle. Physiol. Genomics. 44 (12), 638–650.
Baéza, E., Le Bihan-Duval, E., 2013. Chicken lines divergent for low or high abdominal fat deposition: a relevant model to study the regulation of energy metabolism. Animal. 7 (6), 965–973.
Bartel, DP., 2004. MicroRNAs: genomics, biogenesis, mechanism, and function. Cell 116 (2), 281–297.
Bhaskaran, M., Mohan, M., 2014. MicroRNAs: history, biogenesis, and their evolving role in animal development and disease. Vet. Pathol. 51 (4).
Bockaert, J., Pin, JP., 1999. Molecular tinkering of G protein-coupled receptors: an evolutionary success. EMBO J. 18 (7), 1723–1729.
Buckbinder, L., Talbott, R., Seizinger, B.R., Kley, N., 1994. Gene regulation by temperature-sensitive p53 mutants: identification of p53. Proc. Natl. Acad. Sci. u S. a 91 (22), 10640–10644.
Cai, B., Ma, M., Chen, B., Li, Z., Abdalla, B.A., Nie, Q., Zhang, X., 2018. MiR-16-5p targets SESN1 to regulate the p53 signaling pathway, affecting myoblast proliferation and apoptosis, and is involved in myoblast differentiation. Cell Death. Dis. 9 (3), 367.
Cangelosi, A.L., Puszynska, A.M., Roberts, J.M., Armani, A., Nguyen, T.P., Spinelli, J.B., Kunchok, T., Wang, B., Chan, S.H., Lewis, C.A., Comb, W.C., Bell, G.W., Helman, A., Sabatini, D.M., 2022. Zonated leucine sensing by Sestrin-mTORC1 in the liver controls the response to dietary leucine. Science (1979) 377 (6601), 47–56.
Chen, J.L., Zhao, G.P., Zheng, M.Q., Wen, J., Yang, N., 2008. Estimation of genetic parameters for contents of intramuscular fat and inosine-5′-monophosphate and carcass traits in Chinese Beijing-You chickens. Poult. Sci. 87 (6), 1098–1104.
Chen, X., Ouyang, H., Wang, Z., Chen, B., Nie, Q., 2018. A novel circular RNA generated by FGFR2 gene promotes myoblast proliferation and differentiation by sponging miR-133a-5p and miR-29b-1-5p. Cells 7 (11), 199.
Chen, Y., Wang, X., 2020. miRDB: an online database for prediction of functional microRNA targets. Nucleic. Acids. Res. 48 (D1), D127–D131.
Chen, Y., Wang, Z., Chen, X., Peng, X., Nie, Q., 2021. CircNFIC balances inflammation and apoptosis by sponging miR-30e-3p and regulating DENND1B expression. Genes 12 (11), 1829.
Chen, Y., Zhao, Y., Jin, W., Li, Y., Zhang, Y., Ma, X., Sun, G., Han, R., Tian, Y., Li, H., Kang, X., Li, G., 2019. MicroRNAs and their regulatory networks in Chinese Gushi chicken abdominal adipose tissue during postnatal late development. BMC. Genomics. 20 (1), 778.
Cordani, M., Butera, G., Dando, I., Torrens-Mas, M., Butturini, E., Pacchiana, R., Oppici, E., Cavallini, C., Gasperini, S., Tamassia, N., Nadal-Serrano, M., Coan, M., Rossi, D., Gaidano, G., Caraglia, M., Mariotto, S., Spizzo, R., Roca, P., Oliver, J., Scupoli, M.T., Donadelli, M., 2018. Mutant p53 blocks SESN1/AMPK/PGC-1α/UCP2 axis increasing mitochondrial O2·- production in cancer cells. Br. J. Cancer 119 (8), 994–1008.
Correia de Sousa, M., Gjorgjieva, M., Dolicka, D., Sobolewski, C., Foti, M., 2019. Deciphering miRNAs' Action through miRNA editing. Int. J. Mol. Sci. 20 (24), 6249.
Davoli, R., Luise, D., Mingazzini, V., Zambonelli, P., Braglia, S., Serra, A., Russo, V., 2016. Genome-wide study on intramuscular fat in Italian large white pig breed using the PorcineSNP60 BeadChip. J. Animal Breed. Gene. 133 (4), 277–282.
Fu, S., Zhao, Y., Li, Y., Li, G., Chen, Y., Li, Z., Sun, G., Li, H., Kang, X., Yan, F., 2018. Characterization of miRNA transcriptome profiles related to breast muscle development and intramuscular fat deposition in chickens. J. Cell Biochem. 119 (8), 7063–7079.
Gao, F., Zhao, Y., Zhang, B., Xiao, C., Sun, Z., Gao, Y., Dou, X., 2022. Forkhead box protein 1 transcriptionally activates sestrin1 to alleviate oxidized low-density lipoprotein-induced inflammation and lipid accumulation in macrophages. Bioengineered. 13 (2), 2917–2926.
Geng, C., Xue, Y., Yang, J.H., Gao, M.Y., Zhao, W., Li, C.M., Xie, X.H., Zhang, W.H., Zhang, H.B., Fang, F., Yao, H., Liu, X.J., 2022. SIRT1 Mediates Sestrin1-induced improvement in hepatic insulin resistance. Biomed. Environ. Sci. 35 (1), 79–83.
Georgiadi, A., Lopez-Salazar, V., Merahbi, R.E., Karikari, R.A., Ma, X., Mourão, A., Klepac, K., Bühler, L., Alfaro, A.J., Kaczmarek, I., Linford, A., Bosma, M., Shilkova, O., Ritvos, O., Nakamura, N., Hirose, S., Lassi, M., Teperino, R., Machado, J., Scheideler, M., Herzig, S., 2021. Orphan GPR116 mediates the insulin sensitizing effects of the hepatokine FNDC4 in adipose tissue. Nat. Commun. 12 (1), 2999.
Gjorgjieva, M., Sobolewski, C., Dolicka, D., Correia de Sousa, M., Foti, M., 2019. miRNAs and NAFLD: from pathophysiology to therapy. Gut, 68 (11), 2065–2079.
Himly, M., Foster, D.N., Bottoli, I., Iacovoni, J.S., Vogt, P.K., 1998. The DF-1 chicken fibroblast cell line: transformation induced by diverse oncogenes and cell death resulting from infection by avian leukosis viruses. Virology. 248 (2), 295–304.
Huang, J., Zhao, L., Xing, L., Chen, D., 2010. MicroRNA-204 regulates Runx2 protein expression and mesenchymal progenitor cell differentiation. Stem Cells 28 (2), 357–364.
Huang, R., Zhang, Y., Han, B., Bai, Y., Zhou, R., Gan, G., Chao, J., Hu, G., Yao, H., 2017. Circular RNA HIPK2 regulates astrocyte activation via cooperation of autophagy and ER stress by targeting MIR124-2HG. Autophagy. 13 (10), 1722–1741.
Huang, S., Wang, S., Bian, C., Yang, Z., Zhou, H., Zeng, Y., Li, H., Han, Q., Zhao, R.C., 2012. Upregulation of miR-22 promotes osteogenic differentiation and inhibits adipogenic differentiation of human adipose tissue-derived mesenchymal stem cells by repressing HDAC6 protein expression. Stem Cells Dev. 21 (13), 2531–2540.
Jin, Q., Zhang, F., Yan, T., Liu, Z., Wang, C., Ge, X., Zhai, Q., 2010. C/EBPalpha regulates SIRT1 expression during adipogenesis. Cell Res. 20 (4), 470–479.
Jin, W., Zhao, Y., Zhai, B., Li, Y., Fan, S., Yuan, P., Sun, G., Jiang, R., Wang, Y., Liu, X., Tian, Y., Kang, X., Li, G., 2021. Characteristics and expression profiles of circRNAs during abdominal adipose tissue development in Chinese Gushi chickens. PLoS. One 16 (4), e0249288.
Krüger, J., Rehmsmeier, M., 2006. RNAhybrid: microRNA target prediction easy, fast and flexible. Nucleic. Acids. Res. 34, W451–W454 (Web Server issue).
Lee, J.H., Budanov, A.V., Talukdar, S., Park, E.J., Park, H.L., Park, H.W., Bandyopadhyay, G., Li, N., Aghajan, M., Jang, I., Wolfe, A.M., Perkins, G.A., Ellisman, M.H., Bier, E., Scadeng, M., Foretz, M., Viollet, B., Olefsky, J., Karin, M., 2012. Maintenance of metabolic homeostasis by Sestrin2 and Sestrin3. Cell Metab. 16 (3), 311–321.
Liu, C.X., Chen, L.L., 2022. Circular RNAs: characterization, cellular roles, and applications. Cell 185 (12), 2016–2034.
Maag, J.L.V, 2018. gganatogram: an R package for modular visualisation of anatograms and tissues based on ggplot2. F1000Res. 7, 1576.
Marion-Letellier, R., Savoye, G., Ghosh, S., 2016. Fatty acids, eicosanoids and PPAR gamma. Eur. J. Pharmacol. 785, 44–49.
Milićević, D., Vranić, D., Mašić, Z., Parunović, N., Trbović, D., Nedeljković-Trailović, J., Petrović, Z., 2014. The role of total fats, saturated/unsaturated fatty acids and cholesterol content in chicken meat as cardiovascular risk factors. Lipids Health Dis. 13, 42.
Moreira, G.C.M., Boschiero, C., Cesar, A.S.M., Reecy, J.M., Godoy, T.F., Pértille, F., Ledur, M.C., Moura, A.S.A.M.T., Garrick, D.J., Coutinho, L.L., 2018. Integration of genome wide association studies and whole genome sequencing provides novel insights into fat deposition in chicken. Sci. Rep. 8 (1), 16222.
O'Rourke, J.R., Swanson, M.S., Harfe, B.D., 2006. MicroRNAs in mammalian development and tumorigenesis. Birth Defects Res. Part C Embryo today Rev. 78 (2), 172–179.
Panda, A.C., 2018. Circular RNAs act as miRNA sponges. Adv. Exp. Med. Biol. 1087, 67–79.
Patop, I.L., Wüst, S., Kadener, S., 2019. Past, present, and future of circRNAs. EMBO J. 38 (16), e100836.
Peeters, H., Voz, M.L., Verschueren, K., De Cat, B., Pendeville, H., Thienpont, B., Schellens, A., Belmont, J.W., David, G., Van De Ven, W.J., Fryns, J.P., Gewillig, M., Huylebroeck, D., Peers, B., Devriendt, K., 2006. Sesn1 is a novel gene for left-right asymmetry and mediating nodal signaling. Hum. Mol. Genet. 15 (22), 3369–3377.
Price, N.L., Fernández-Hernando, C., 2016. miRNA regulation of white and brown adipose tissue differentiation and function. Biochim. Biophys. Acta 1861 (12 Pt B), 2104–2110.
Shang, Z., Guo, L., Wang, N., Shi, H., Wang, Y., Li, H., 2014. Oleate promotes differentiation of chicken primary preadipocytes in vitro. Biosci. Rep. 34 (1), e00093.
Shao, F., Wang, X., Yu, J., Jiang, H., Zhu, B., Gu, Z., 2014. Expression of miR-33 from an SREBF2 intron targets the FTO gene in the chicken. PLoS. One 9 (3), e91236.

Shen, L., Gan, M., Li, Q., Wang, J., Li, X., Zhang, S., Zhu, L., 2018. MicroRNA-200b regulates preadipocyte proliferation and differentiation by targeting KLF4. Biomed. Pharmacother. 103, 1538–1544.
Song, Y., Tran, M., Wang, L., Shin, D.J., Wu, J., 2022. MiR-200c-3p targets SESN1 and represses the IL-6/AKT loop to prevent cholangiocyte activation and cholestatic liver fibrosis. Lab. Invest. 102 (5), 485–493.
Sun, T., Fu, M., Bookout, A.L., Kliewer, S.A., Mangelsdorf, D.J., 2009. MicroRNA let-7 regulates 3T3-L1 adipogenesis. Mol. Endocrinol 23 (6), 925–931.
Song, T., Zhang, X., Wang, C., Wu, Y., Dong, J., Gao, J., Cai, W., Hong, B., 2011. Expression of miR-143 reduces growth and migration of human bladder carcinoma cells by targeting cyclooxygenase-2. Asian Pacific journal of cancer prevention. APJCP 12 (4), 929–933.
Wang, Q., Li, Y.C., Wang, J., Kong, J., Qi, Y., Quigg, R.J., Li, X., 2008. miR-17-92 cluster accelerates adipocyte differentiation by negatively regulating tumor-suppressor Rb2/p130. Proc. Natl. Acad. Sci. u S. a 105 (8), 2889–2894.
Wang, X.W., Heegaard, N.H., Orum, H., 2012. MicroRNAs in liver disease. Gastroenterology 142 (7), 1431–1443.
Xu, P., Vernooy, S.Y., Guo, M., Hay, B.A., 2003. The Drosophila microRNA Mir-14 suppresses cell death and is required for normal fat metabolism. Curr. Biol. 13 (9), 790–795.
Yang, J., Cheng, M., Gu, B., Wang, J., Yan, S., Xu, D., 2020. CircRNA_09505 aggravates inflammation and joint damage in collagen-induced arthritis mice via miR-6089/AKT1/NF-κb axis. Cell Death. Dis. 11 (10), 833.
Yu, C.Y., Li, T.C., Wu, Y.Y., Yeh, C.H., Chiang, W., Chuang, C.Y., Kuo, H.C., 2017. The circular RNA circBIRC6 participates in the molecular circuitry controlling human pluripotency. Nat. Commun. 8 (1), 1149.
Yu, G., Wang, L.G., Han, Y., He, Q.Y., 2012. clusterProfiler: an R package for comparing biological themes among gene clusters. OMICS. 16 (5), 284–287.
Yuan, P., Zhao, Y., Li, H., Li, S., Fan, S., Zhai, B., Li, Y., Han, R., Liu, X., Tian, Y., Kang, X., Zhang, Y., Li, G., 2022. CircRNAs related to breast muscle development and their interaction regulatory network in Gushi Chicken. Genes. (Basel) 13 (11), 1974.
Zaidman, N.A., Tomilin, V.N., Hassanzadeh Khayyat, N., Damarla, M., Tidmore, J., Capen, D.E., Brown, D., Pochynyuk, O.M., Pluznick, J.L., 2020. Adhesion-GPCR Gpr116 (ADGRF5) expression inhibits renal acid secretion. Proc. Natl. Acad. Sci. u S. a 117 (42), 26470–26481.
Zamkova, M., Khromova, N., Kopnin, B.P., Kopnin, P., 2013. Ras-induced ROS upregulation affecting cell proliferation is connected with cell type-specific alterations of HSF1/SESN3/p21Cip1/WAF1 pathways. Cell Cycle 12 (5), 826–836.
Zhai, B., Li, H., Li, S., Gu, J., Zhang, H., Zhang, Y., Li, H., Tian, Y., Li, G., Wang, Y., 2023. Transcriptome analysis reveals FABP5 as a key player in the development of chicken abdominal fat, regulated by miR-122-5p targeting. BMC. Genomics. 24 (1), 386.
Zhang, C., Ren, L., Zhang, H., Yang, S., Deng, M., He, L., Cao, R., Zhao, C., Xia, J., 2022. SESN1, negatively regulated by miR-377-3p, suppresses invasive growth of head and neck squamous cell carcinoma by interaction with SMAD3. Hum. Cell 35 (4), 1100–1113.